The Surface Structure Analysis of a Heat-treated Metal/Si System by a Quantitative Auger Electron Spectroscopy Method

by

Katsumi NISHIMORI, Heizo TOKUTAKA, Masashi MASUDA
and Naganori ISHIHARA

Department of Electronics

(Received September 1, 1988)

When a system of a Au, Cu or Pd thin film deposited on a Si (100) substrate is heat-treated, various metal-silicide phases are formed on the Si substrate. The thicknesses and elemental compositions of these silicides segregated onto the surface region were determined analytically by a quantitative Auger electron spectroscopy (AES) method, without destroying the system. The AES data were numerically processed by the micro-computer controlled AES apparatus, so that the accuracy of the measurements was improved. In the three metal/Si systems, we carried out the AES measurements for the interaction between the metal (Au, Cu or Pd) and Si at the surface and interface when the system was heat-treated from 100°C to 1000°C. The models obtained from our analysis can provide useful information to the formation of metal-silicides and metal-silicon interfaces of the heat-treated systems.

Key words : Auger electron spectroscopy, Quantitative analysis, Surface structure, Surface composition, Au/Si, Cu/Si, Pd/Si, Metal silicide, Data processing with micro-computer.

1. Introduction

Auger electron spectroscopy is the method most commonly used to determine the elemental composition of a solid surface. To upgrade the ability of this method, we have developed a new quantitative analytical approach for AES measurements [1-5], by which it is possible to explain the AES experimental results of the monolayer over-growth [1,2], the surface segregation of a binary alloy [3,4] and the alloy formation of Si with a metal when the system is heat-treated [5]. For a system of metal overlayer on Si substrate, it has been reported that metal-Si interaction occurs at the interface, through which metal atoms and/or Si atoms go in and out to each other [6-9]. In this compound formation with both Si and a metal, the major interests are in identifying the various phases formed and in measuring their growths as a function of heat-treatment temperature or time. In order to investigate these problems, several MeV ion backscattering and AES measurements combined with ion sputtering are widely used. However, for layer thicknesses less than ∿200 A, measurements by ion backscattering is difficult. The depth profile technique by AES combined with ion sputtering is completely destructive. The quantitative determination of the surface composition during the depth profile suffers from a preferential sputtering effect [10] due to the different sputtering yields of Si and a metal.

In this article, three systems of Au, Cu and Pd thin film (100∿200 Å) on Si (100) substrates have been investigated by our quantitative AES method. Using this method, it is possible to determine the surface or interface structure and the elemental composition of a segregated binary alloy layer of a metal-Si system without destroying the surface and the interface. Each of these three systems is sequentially heat-treated in the same vacuum with increasing heat-treatment temperature or time.

The result of the quantitative AES analysis which is reported here gives us a more advanced understanding of the nature of these interfacial regions.

2. Experimental

2.1. Sample preparation.

A mirror-polished n-type Si(100) substrate of 2∿3 ohm cm resistivity was used in all experiments. The Si substrate was chemically etched with a 6:1:2 volume ratio of HNO :HF:acetic acid, respectively. The dimension of the substrate was 13x5x0.35 mm. The Si substrate was clamped between two tantalum strips and cleaned in an ultra-high vacuum ($<10^{-9}$ Torr) by heating it to temperature of about 1200 °C. Heating was achieved by passing a

current directly through the Si crystal. Also, in order to decrease the out-gas from the sample holder, the heat-cleaning procedure was repeated several times. For annealing or heat treatment of Si substrate, the temperature versus the passing current was calibrated using a chromel-alumel thermocouple on the Si substrate in a conventional high vacuum.

The deposition of each metal (Au, Cu or Pd) on a Si substrate was made by a resistive heating of W filament (for Au and Pd) or Ta filament (for Cu) in an ultra-high vacuum. The shield box surrounding the evaporation filament was heated by the W heater stretched around the inside of the box. To avoid contamination of the sample during the metal evaporation, heating of the box was continued at a temperature of 400∿500°C, until the pressure of the UHV chamber became less than $7 \sim 8\times10^{-10}$ Torr. The pressure during each metal deposition was less than 1×10^{-9} Torr. The deposition rates of Au, Cu and Pd were 60, 70 and 15 Å/min., respectively.

Auger data were acquired with a single-pass cylindrical mirror energy analyzer (CMA; Varian, model 981-2607). Primary beam energy of 2.5 keV was used and the beam current of 10 μA was controlled by the electron gun power supply, using which the beam current variation was less than 1%. This CMA measurement system was controlled by the micro-processor units (MPU) and the CMA Auger signal was digitally processed for the quantitative data acquisition.

2.2. Data acquisition.

The block diagram of the system is shown in Fig. 1. The system consists of the measurement unit and the main system.

2.2.1. Measurement unit.

The programable sweep voltage supply is controlled by the command signals from MPU (MC 6809) and provides the CMA analyzing voltage which is required. Auger signals from CMA are differentiated by passing through the phase sensitive detection (PSD) circuit of a lock-in amplifier. The Auger signals are converted into digital signals, and then stored in the memory circuits of the MPU. These Auger signals are transmitted to the main system, as soon as scanning of the CMA analyzing voltage is finished.

2.2.2. Main system.

The main system has the following four functions.

i) The control of the measurement unit according to the initial set up of AES measuring conditions.

ii) The processing of the Auger data transmitted from the measurement unit.

iii) The display of the Auger spectrum on an oscilloscope or an X-Y recorder.

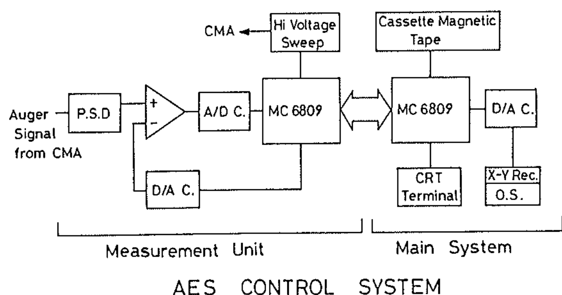

Fig. 1. AES control system for quantitative Auger measurements.

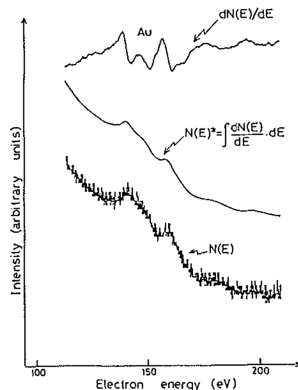

Fig. 2. Differentiated dN(E)/dE and undifferentiated N(E) Auger spectra of 200 Å Au film on Si(100) substrate.

iv) The store of Auger data on cassette tapes or floppy disks.

The data processing of ii) has four further functions as follows:

1) Numerical output of Auger data.

2) Auger peak searching in the differentiated spectra dN(E)/dE.

3) Numerical integration of the spectra dN(E)/dE. The spectra obtained by this numerical integration are expressed as N*(E).

4) Numerical calculation of the Auger peak area on the integrated spectrum N*(E).

In fig. 2, there are two kinds of undifferentiated Auger spectra which are N*(E) and N(E). The N*(E) spectrum of the Au Auger peaks (∿ 150 eV) in the energy region of 100 ∿200 eV is obtained by the above described signal procedure (3). The N(E) spectrum was obtained by the direct measurement of the CMA current output from the electron multiplier with a high common mode voltage isolation amplifier. When the N*(E) spectrum is compared with the N(E), we can point out the following four results:

a) In spite of the complicated feature of the secondary electron distribution in this energy region, the N*(E) reproduces the N(E) curve very well.

b) The signal to noise ratio S/N of the integrated spectrum N*(E) is much larger than that of the N(E) spectrum.

c) Since both spectra of dN(E)/dE and N*(E) are digitally processed with MPU, the energy values E of both spectra coincide completely with each other.
d) As the integrated spectrum N*(E) is used in place of the spectrum N(E), the measurement of the N(E) spectrum is not necessary. Then, the measurement times required in all AES experiments are made shorter.

For the above reasons we use the integrated spectra N*(E) instead of the spectra N(E) in our later AES experiments.

2.3. A procedure for determination of the Auger peak intensity on the N*(E) spectrum.

The Auger current associated with a given transition is $I_A=\int[N(E)-Nb(E)]dE$, where Nb is the background and the interval of the integration covers the extent of the peak [11]. When chemical reaction, e.g. oxidation, occurs in the surface region of solids, the Auger line of reacted atoms which is measured in N(E) mode changes in the peak energy location and the line shape. For metal-Si systems, it was reported [10] that the line shape of Si LVV Auger transition which contains the Si valence band (V) changes owing to the formation of metal-silicide. However, photoemission and Auger electron spectroscopic measurements of the Ni on Si system [12] showed that, although the Ni-Si reaction occurs at the interface, the change of Si LVV Auger peak height in N(E) spectrum gives us a good measure of Ni exposure as well as the change of Ni 3d peak intensity in photoemission spectrum does. Also, in Pd/Si system, Schmid et al. [9] determined the composition and the thickness of the surface layer which is formed as a result of Pd-Si reaction at the interface. In their quantitative analysis, they used the integrated intensity of Si LVV Auger peak in N(E) spectrum. Therefore, in most metal-Si systems, the integrated Auger intensity can be used for a quantitative analysis when the line shape change due to the formation of metal-silicides exists. In the electron energy region lower than 100 eV, the Auger electron current is very small relative to the background current of secondary electrons from solid surface, as shown in fig. 6. Since the background function Nb(E) is not clearly defined in general, the above integration $\int[N(E)-Nb(E)]dE$ is very difficult to perform. However, Ishiguro and Homma proposed a simple and useful method [13] in relation to this integration. By this method, they treated quantitatively the Auger peak intensity ratio of metal oxides. Their method is applied to a case of our AES measurements, and the result is shown in fig. 3. The figure shows the dN(E)/dE spectra and N(E) spectra of Si LVV Auger peaks obtained from the surfaces of a clean Si substrate and a 10 Å Cu thin film deposited on Si substrate at room temperature. According to their method, in

the case of a clean Si, the two points on the N(E) curve of Si LVV Auger peak are chosen by two energy values of maximum (88 eV) and minimum (92 eV) on the Si LVV dN(E)/dE curve of clean Si.

These two points are connected by a straight line. Then, the area surrounded by the N(E) curve and the straight line is numerically calculated as a Si LVV Auger current I_A. In the case of a 10 Å Cu thin film on a Si substrate, the dN(E)/dE spectrum of a Si LVV Auger peak shows a complicated peak shape due to the formation of Cu-silicide, as shown in fig. 3. However, the Auger current in this case can also be calculated by the above procedure used for the case of the clean Si substrate. In this case the two energy values of maximum and minimum on the dN(E)/dE curve of fig. 3 are taken as 88 eV and 94 eV, respectively. Then, two points on the N(E) curve are chosen by these two energy values. As described in the next section, our quantitative AES method needs the normalized Auger currents. The normalization of Auger currents is made by using these Auger peak areas Ai. For example, when Ax is the area of Si LVV Auger peak obtained from the surface of a Cu thin film on a Si substrate, it is divided by the area Asi of Si LVV Auger peak obtained from the clean Si substrate. The normalized Si LVV Auger current for the Cu thin film on Si is expressed as Ax/Asi. In the system of a metal (Au, Cu or Pd) thin film on a Si substrate, the normalized

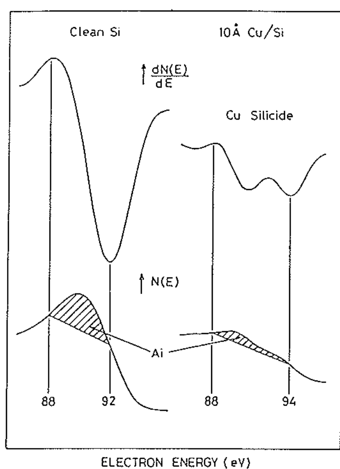

Fig. 3. Determination of Auger currents of Si LVV peaks from clean Si substrate and 10 Å Cu on Si (Cu-silicide).

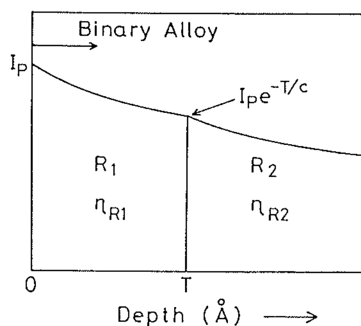

Fig. 4. A schematic model of a binary alloy system having a surface segregation region of the solute atom composition R1 and thickness T, when R2 is the solute atom composition of the bulk alloy.
Ip: primary beam current,
η_{R1}, η_{R2} : secondary electron yields.

Auger currents from a metal and Si are also determined by using the above normalizing procedure.

3. Analyzing model (Theory).

The quantitative AES method used in this paper is the same method that has been described in detail in references [1∿5], where all the surface structures are simply considered as layered structures for the cases of a monolayer over-growth [1,2], a surface segregation of a binary alloy [3,4] and a surface reaction of the Ag-Si or Au-Si system [5]. In the case of a Ag-Si or Au-Si system, the change of the interface after heat-treatment has been analyzed successfully. This method provides the quantitative formalism to calculate the yield of Auger electrons produced by the primary electron, forward- and back-scattered secondary electrons in the layer materials. The number of the layers with different compositions is taken as two in order to simplify the analysis. The model (two layer model) is shown in fig. 4. If the solute atom composition R2 in the bulk (or the solute atom composition R1 in the surface-segregated layer) is known, the number of unknown parameters is just two of the thickness T and the composition R1 of the surface-segregated layer (or the composition R2 of the bulk). Our

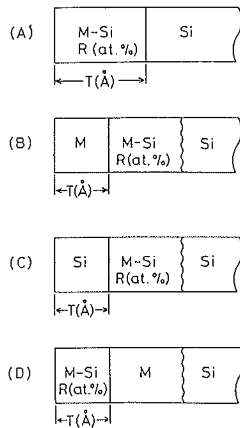

Fig. 5. Proposed structure models after heat-treatment of M(metal)/Si systems. R represents metal composition of M-Si alloyed layer.

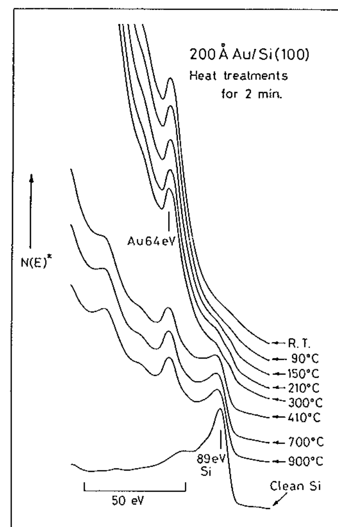

Fig. 6. Numerically integrated N*(E) spectra of 200 Å Au film on Si (100) substrate after heat-treatments at various temperatures for 2 min..

quantitative AES method can also be developed for the system with three different layers to be analyzed (three layer model). However, since the analysis based on the three layer model is beyond the purpose of this paper, it is not discussed here.

Let us apply the two layer model (fig. 4) to the system of a metal (Au, Cu or Pd) overlayer on a Si substrate when the system is heat-treated. The four models shown in fig. 5 are all that can be considered for the system. In each of these four models, the two unknown parameters are the metal atom composition R (at. %) in the binary alloy layer and the thickness T (Å) of surface-segregated layer. It is assumed that the Si substrates in the models B, C and D of fig. 5 are in the bulk and they are far from the surfaces to be analyzed.

Using the result of our quantitative AES method [4,5], the two normalized Auger signals I_M and Isi from metal atoms and Si atoms are expressed as follows:

$$I_M = I_M(T, R), \qquad \text{--- (1)}$$

$$Isi = Isi(T, 100-R), \qquad \text{--- (2)}$$

respectively. When we replace the left hand sides of the equations of (1) and (2) with the two normalized Auger signals of I_M and Isi, respectively, obtained from the quantitative Auger measurements, the two unknown parameters

Table 1. Physical values necessary for the analysis of the results by the heat-treatment of metal/Si systems[a].

Metal/Si system	Electron energy (eV)		0.74xℓ(E) (Å)	ℓ(E) (Å)	η	α
Au/Si	Au Auger	240	Au[b] 6.2			
			Si 6.4			
	E_{AV}(Au)[c]	1365	Au 16.3		η_S 0.591	Au 2.392
		1464	Si 46.6		η_B 0.274	Si 2.374
	Si Auger	92	Au 5.0			
			Si 5.0			
	E_{AV}(Si)	1234	Au 15.3		η_B 0.696	Au 3.321
		1366	Si 42.6		η_S 0.320	Si 3.106
	E_p	2500		Au 32.6		
				Si 127.6		
Cu/Si	Cu Auger	920	Cu 16.0			
			Si 25.3			
	E_{AV}(Cu)	1706	Cu 27.3		η_S 0.350	Cu 1.398
		1733	Si 58.3		η_B 0.206	Si 1.433
	Si Auger	92	Cu 5.0			
			Si 5.0			
	E_{AV}(Si)	1281	Cu 21.3		η_B 0.560	Cu 3.242
		1366	Si 42.6		η_S 0.320	Si 3.106
	E_p	2500		Cu 51.5		
				Si 127.6		
Pd/Si	Pd Auger	330	Pd 6.8			
			Si 7.0			
	E_{AV}(Pd)	1383	Pd 20.1		η_S 0.466	Pd 2.387
		1461	Si 46.5		η_B 0.274	Si 2.373
	Si Auger	92	Pd 5.0			
			Si 5.0			
	E_{AV}(Si)	1263	Pd 18.7		η_B 0.536	Pd 3.271
		1366	Si 42.6		η_S 0.320	Si 3.106
	E_p	2500		Pd 43.2		
				Si 127.6		

[a] All values are defined clearly in refs. [1-5].
0.74xℓ(E): electron escape depth,
ℓ(E): electron mean free path,
η_B, η_S: secondary electron yield in base or solute metal,
$\alpha = \beta\Phi(E_{AV}) / \Phi(E_p)$,
β: geometrical factor [29].
$\Phi(E)$: Gryzinski ionization cross section [30].

[b] Escape depth through the material shown.

[c] E_{AV}(Au) is the averaged energy of the secondary electrons having enough energy to produce Au Auger electrons.

of R and T can easily be solved analytically as a unique solution.

In fact, for the two values of I_M and Isi of equations (1) and (2), we have used the two measured Auger signals of a metal and Si. These signals are normalized by the procedure outlined in the previous section. The physical values necessary for our analysis are all tabulated in table 1. These values are obtained in the same manner as described in references 4 and 5. The methods to get precisely these values are described in reference 14.

Using our theory, we can find out the model corresponding to a real metal/Si system after heat-treatment, which becomes one of the four models of fig. 5. Thus, we can determine the thickness as well as the composition of the metal-Si alloyed layer.

4. Results and discussion.

In this section we show and discuss the results obtained by our analytical method which is applied to the quantitative Auger measurements of the three metal/Si systems (Au/Si, Cu/Si and Pd/Si).

Since these Auger measurements in the low energy region suffer from the presence of a steep background due to a secondary electron emission containing the low energy Auger electron signals of Au 69 eV, Cu 60 eV or Pd 43 eV, these Auger signals are not employed in our quantitative analytical method. However, the change of these Auger peak shapes due to the sequential heat-treatments is shown in each Auger spectrum, in order to compare it qualitatively with the change of Si LVV Auger peak shapes. The Si KLL Auger peak in the very high energy region is not employed in our quantitative AES measurements because it is less sensitive.

4.1. Au/Si.

The Au thin film of 200 Å was deposited on the Si(100) substrate at room temperature. This Au/Si system was sequentially heat-treated with an increasing heat-treatment temperature for the constant heat-treatment time of 2 min. by the resistive heating of the Si substrate. Figs. 6 and 7 show the changes of the Auger spectra N*(E) and dN(E)/dE, respectively, in this Au/Si system when heat-treated. In the dN(E)/dE spectrum of 300°C of fig. 7, we can clearly see that the 92 eV Si LVV peak splits into the two peaks (the double peak) located at 90 eV and 95 eV. Such double peak features are also seen in the case of lower heat-treatment temperatures than 300°C and the peak height gradually becomes larger with increasing temperature up to 300°C. The Si double peaks characterize the metastable Au-silicide formed on the surface of the heat-treated Au/Si system [15].

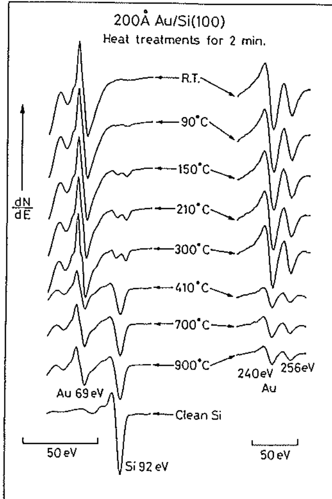

Fig. 7. Auger spectra taken from 200 Å Au/Si specimen at successive stages of the heat-treatment.

Fig. 8.→ Result of the analysis for 200 Å Au/Si system in fig. 7.

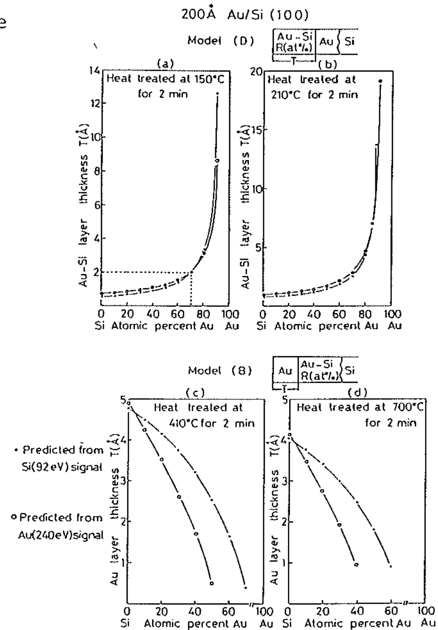

At the higher heat-treatment temperature, the double peak of Si LVV changes into a single peak. At the same time other Auger peaks of Au (69 eV) and Au (240 eV) suddenly decrease in their peak heights (see the spectrum of 410°C in fig. 7). This sudden change of the spectra occurs in the narrow temperature range of 310 ±3°C [5]. The change is also observed by the sudden change in the backgrounds of the N*(E) at a heat-treatment temperature from 300 to 410°C, as shown in fig. 6. Little changes exist in the dN(E)/dE and N*(E) spectra at the higher heat-treatment temperatures from 410 up to 900°C. A more stable Au-Si interface will be formed in these heat-treatment stages.

The Auger signals used for our analysis are the Si LVV (92 eV) and Au (240 eV) peaks. Each of the normalized Auger signals was obtained by numerical integration on the N*(E) curves according to the procedure described in the section 2.3.. The results of our analysis are shown in fig. 8. As mentioned in section 3, a unique solution can be obtained as the crossing point of the two curves in the graph (a), (b), (c) or (d) in this figure. One of the two curves is obtained from the Si LVV Auger signal and the other is the curve obtained from the Au (240 eV) signal in each of the four graphs. In the result of our analysis for the heat-treatment of 150 °C, a unique solution, or the crossing point of the

curves, exists only for model (D), and there are no solutions for any other models. This solution is shown in graph (a) of fig. 8, with the model (D). In this graph (a), the abscissa shows Au atom composition R (at.%) in the Au-Si alloy of the topmost layer of model (D) and the ordinate shows the thickness T (Å) Of this Au-Si alloyed layer. Therefore, the crossing point of these two curves gives us only the solution of R(Au)=70 at.% and T=2 Å. The pure Au layer beneath this Au-Si alloyed layer is too thick to be analyzed by our method. In the result (b) of heat-treatment at 210°C, model (D) also has the solution of R(Au)=85 at.% and T=7 Å, the values of which become larger than those of the above result (a). The results (not shown in this paper) for heat-treatments up to 300°C are similar to the result of 210°C.

However, in a heat-treatment temperature higher than 410 °C, we have obtained a unique solution for model (B) as shown in graphs (c) and (d) of fig. 8, but no solutions exist for any other models. In these graphs (c) and (d), the ordinates show the pure Au film thickness T of the topmost layer and the abscissas show the Au atom composition R(Au) in a Au-Si alloyed layer beneath the topmost Au layer. In each of these two graphs (c) and (d), the crossing point of these two curves also shows a unique solution for model (B). The pure Au film thickness T decreases gradually with increasing heat-treatment temperature as 4.7 Å for 410°C and 4.0 Å for 700°C. The thickness T, however, does not change for the heat-treatments at higher temperatures from 700°C up to 900°C. The Au composition of the alloyed layer beneath the Au layer is less than R(Au)=3 at.% for each heat-treatment at a temperature higher than 410°C. The alloyed layer is very close to the pure Si substrate.

Thus, it must be noticed that when the 200 Å Au/Si system is heat-treated our analysis shows two quite different models, which are model (D) for lower heat-treatment temperature (silicide formed) and model (B) for higher heat-treatment temperature than the surface eutectic point of 310°C [5]. Hiraki et al. [16] reported that Si atoms diffuse from Si substrate through a thick (~900 Å) Au film and segregate onto the Au film at a temperature lower than 200°C. At these lower temperatures, the segregated Si atoms form a thin meta-stable Au-rich silicide layer on a pure Au thick film, which is found by using the AES depth profile technique [17]. These phenomena are in very good agreement with our above result of model (D). Both the thickness and Au composition of the Au-silicide layer gradually increase from T=2 to 7 Å, and from R(Au)=70 to 85 at. %, respectively, with increasing heat-treatment temperatures from 150 to 300°C.

However, model (B) gives us a unique solution when the Au/Si system is

heat-treated at a temperture higher than the surface eutectic point (310°C). This result shows that the pure Au thin layer of 4 ∿5 Å (one to two monolayers) always remains as the topmost layer in spite of the rapid diffusion [6] of a large amount of Au into the bulk Si at these higher heat-treatment temperatures. The interaction between a Au film and a Si (111) substrate at higher temperature than 400°C was investigated by Le Lay et al. [18], who concluded that a Au thin film grows on the Si substrate in Stranski-Krastanov (S-K) mode, i.e. initial Au layer growth followed by the island formation. In the AES data of Le Lay et al. [18], both Auger signals of Au and Si are almost constant against increasing Au covarage of 0 > 1.5. Thus, the contribution of islands to the Au Auger signal seems to be negligible when grown in an S-K mode. It is also reported [19] that the contribution of islands to the Auger signals is almost negligible because of the very small density of Ag islands in the case of a thin Ag film deposited on Si substrate at 500°C. Our analysis is based directly on the ability of AES to detect the population density of the specific element in the surface region. Therefore, our analysis is correct within the analyzing ability of AES, so long as the contribution of the islands to the Auger signal is negligible, even if the Au islands are formed on the topmost Au layer. Then, in our case, for higher heat-treatment temperature than the surface eutectic point, a pure Au thin layer of one to two monolayers can exist stably on the Si substrate, as in the case of other researchers' experiments [20, 21].

4.2. Cu/Si.

A differentiated Si LVV Auger peak splits into the two peaks of 88 and 94 eV due to the Cu-silicide formation as previously shown in fig. 3, when a 10 Å Cu thin film is deposited on Si substrate at room temperature. In fact, this double peak is very similar to that of Si LVV peak of meta-stable Au-silicide formed on the thick Au layer as described in the section 4.1. In order to investigate this Cu-silicide formation in detail, we observed the change of AES spectra due to the heat-treatment at relatively low temperature. A 200 Å Cu film was deposited on the Si substrate at room temperature. This system was then heat-treated in an ultra-high vacuum at the constant temperature of 150 °C with increasing heat-treatment time. Fig.9 shows the change of these AES spectra as a function of heat-treatment time. For a longer heat-treatment time, the Si LVV peak height gradually increases whereas the shape is still the double peak. On the contrary to the Si signal change, Cu Auger peaks of 60 eV and 920 eV gradually decrease in their heights. After 60 min. heat-treatment time, the Si LVV double

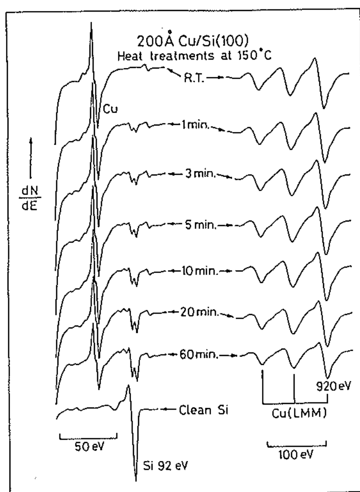

Fig. 9. Auger spectra taken from 200 Å Cu/Si system heat-treated at 150°C for various annealing periods.

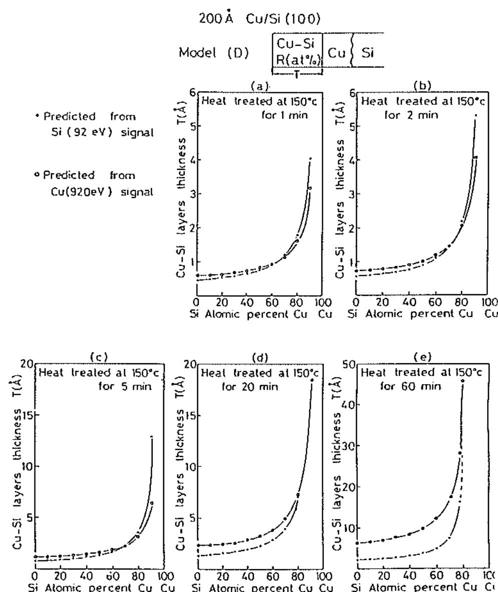

Fig. 10. Result of the analysis for the system in fig. 9.

peak or the 920 eV Cu Auger peak keeps an almost constant height. The Auger signals used for our analysis are the Si LVV peak and Cu Auger peak of 920 eV. The result of the analysis for this case is shown in fig. 10. Model (D) shows a unique solution for all these heat-treatment stages, which is very similar to the case of the Au/Si system as shown in fig. 8 (a) and (b). The result shows that the surface Cu-Si alloyed (Cu silicide) layer exists on the pure thick Cu layer which is also sitting on the Si substrate. The Cu composition and the thickness of the Cu-silicide layer increase from 70 to 80 at.%, and from 1 to 30 Å, respectively, with longer heat-treatment time. The result shows that the Cu-silicide of the topmost layer grows as a function of the heat-treatment time at a relatively low temperature (150°C).

Next, a system of 200 Å Cu film on Si substrate was sequentially heat-treated for 2 min. with an elevating temperature. Fig. 11 shows the change of AES spectra due to these heat-treatments. For a temperature lower than 190°C (the analytical result is not shown in fig. 12), model (D) gives us a unique solution which is very similar to fig. 10. When the Cu/Si system is heat-treated at a higher temperature between 210 and 350°C, the unique solution is no longer obtained from model (D), but only model (C) gives us the solution as shown in the graphs (a) and (b) of fig. 12. In

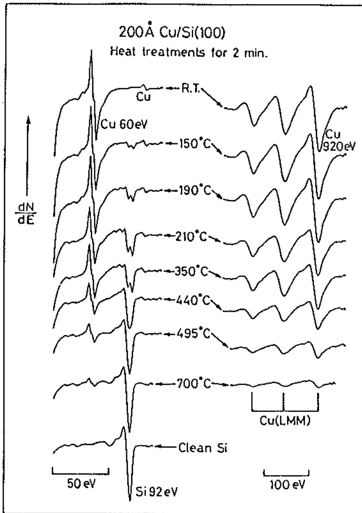

Fig. 11. Auger spectra taken from 200 Å Cu/Si specimen at successive stages of the heat-treatment.

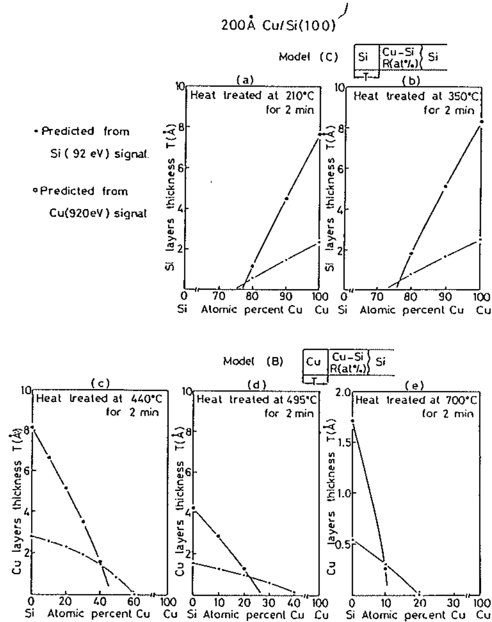

Fig. 12. Result of the analysis for the system in fig. 11.

each of the two graphs, the ordinate expresses the thickness T of the Si segregated layer on the thick layer of Cu-Si alloy which is extended deeply into the Si substrate. The abscissa shows the Cu atom composition R of this Cu-Si alloyed layer. From the graphs (a) and (b) in fig. 12, it follows that the thickness T= 0.5 Å of the Si surface layer is less than 1/4 monolayer (= 2.35/4 Å [22]) and the Cu atom composition R(Cu)=75 at.% of the Cu-Si alloyed thick layer corresponds to the composition of the Cu-silicide of Cu_3Si. The Cu_3Si thick layer is formed stably on the Si substrate during these heat-treatments.

At temperatures higher than 440°C, the Si LVV double peak changes into a single Si LVV Auger peak as shown in fig. 11. After this temperature (440 C), the analyzed model also changed from (C) to (B) as shown in fig. 12. In the fig. 12 (c) (440°C), the thickness of the pure Cu topmost layer is 1.45 Å which is slightly thicker than a half monolayer of Cu (= 2.56/2 Å [22]). It shows that a very thin Cu layer covers the thick Cu-Si alloyed layer of R(Cu)= 42 at.% which extends deeply into the Si substrate. From 495°C to 700°C, the thickness of the topmost Cu layer considerably decreases from 0.9 to 0.3 Å, respectively. The Cu atom composition of the Cu-Si alloyed layer also decreases from 20 to 10 at.%. This phenomenon is very different from the Au/Si case after 410°C (c.f. fig.8 (c) and (d)), whereas

the 4∿5 Å Au topmost layer remains on the almost pure Si substrate. This result reveals that, at a temperature higher than 440°C, a relatively large amount of Si from the substrate successively diffuses into the Cu_3Si layer or the Cu_3Si diffuses into the Si substrate, where the Cu_3Si layer is fully grown around 300°C. In order to break the Cu_3Si silicide, it needs the heat-treatment at over 858°C [23] which is the melting point. Below this temperature, the unit form of Cu Si diffuses into Si or Si diffuses among the Cu_3Si silicides. Therefore, the dense Cu composition still remains in the (B) model of fig. 12 (c), (d) and (e) which is different from Au/Si case of fig. 8 (c) and (d).

4.3. Pd/Si

Fig. 13 shows the change of the differentiated Auger spectra when the system of a 100 Å Pd film on Si (100) substrate was heat-treated at various temperatures for 2 min.. The Si LVV Auger spectrum of 90°C heat-treatment is characterized by the feature with several peaks in the energy range of 80 to 94 eV due to the Pd Si formation in the surface region [24, 25]. No changes of this Si Auger line shape have been observed between 250 and 410°C. At higher temperatures than 450°C, the Si Auger line shape becomes closer to the elemental Si LVV Auger line, increasing its peak height. The

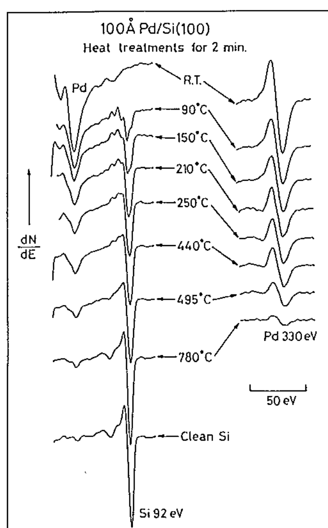

Fig. 13. Auger spectra taken from 100 Å Pd/Si specimen at successive stages of the heat-treatment.

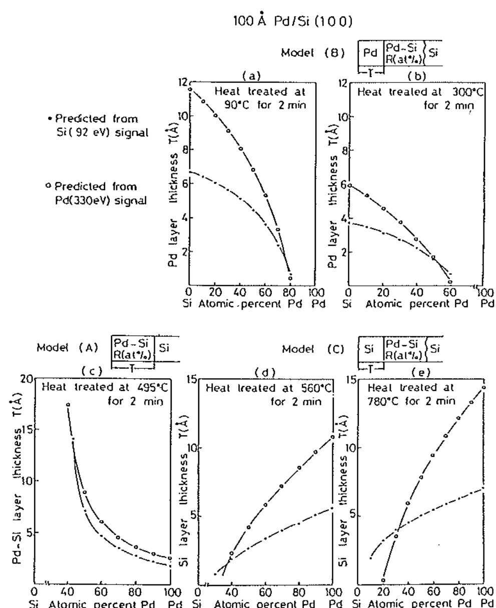

Fig. 14. Result of the analysis for the system in fig. 13.

intensity of Pd (330 eV) Auger peak continues to decrease with elevating temperature. However, the Pd (330 eV) peak height keeps constant in the range from 250 to 410°C.

The Auger signals used for our analysis are the Si LVV (92 eV) Auger line and the Pd 330 eV peak. Fig. 14 shows the result of our analysis for the Pd/Si system. A unique solution was obtained from model (B) for heat-treatment temperatures from 90 to 440°C. However, at 495 °C and at higher temperatures than 560 °C, (A) and (C) models were the solutions, respectively. Then, let us examine the solution by our analysis when the heat-treatment temperature increases. The solution of 90°C is T= 1.2 Å of the topmost Pd layer's thickness and R(Pd)= 77 at.% of the Pd atom composition in the Pd-Si alloyed layer beneath the Pd layer. From 90 to 210°C, the Pd composition of the Pd-Si alloyed layer gradually decreases, taking the same thickness (1.2 Å) as that of the topmost Pd layer for 90°C. However, in the temperature range of 250 to 410 °C, each of those values remains almost constant, that is, the thickness of the topmost Pd layer is 1.6 Å and the Pd composition of Pd-Si alloyed layer is 51 at.% as shown typically in graph (b) (300°C) of fig. 14. For 440°C heat-treatment, the solution of model (B) provides that the Pd composition of the Pd-Si alloyed layer again starts to decrease gradually to 40 at.%, although the thickness of the topmost Pd layer is 1.6 Å which is the same value with 300°C.

As soon as the heat-treatment temperature is elevated up to 495°C, the model giving a unique solution changes from (B) to (A) as shown in graph (c) of fig. 14. In this graph, the solution shows that the topmost Pd layer vanishes and only the Pd-Si alloyed layer is formed as the new topmost layer on the Si substrate with a thickness of 14 Å and a Pd composition of 43 at.%. The thickness of this Pd-Si layer may be considered to be much larger than 14 Å, because the two curves in graph (c) of fig. 14 have a similar steep slope toward the direction of increasing thickness and become very close to each other in the narrow region (composition as the abscissa) where the two curves cross to make a unique solution. At a temperature higher than 495 °C, as shown in graphs (d) and (e) of fig. 14, each of the solutions obtained from model (C) indicates that Si atoms from the substrate segregate to the surface of the Pd-Si alloyed layer through this layer. In the graph (e) for 780°C the thickness of the Si surface-segregated layer increases to 4.2 Å, and the Pd composition of the Pd-Si alloyed layer decreases to 34 at.%. Only one single phase of Pd Si is known to be formed by the reaction between a thin Pd film and a crystalline Si substrate in the temperature range of 200 to 700°C [26, 27]. Recently, it is also reported that Si atoms segregate from the Si substrate to the surface of the Pd_2Si

layer at a heat-treatment temperature higher than 400°C [25, 28]. Thus, our above result agrees very well with these observations by other experimental methods. That is, with heat-treatments from 90 to 210 °C, a thicker Pd overlayer may be transformed completely into a Pd_2Si layer. At heat-treatments over 250°C, the formed Pd-silicide is diluted with Si atoms which are supplied from the Si substrate (see the graphs (b)-(e) of fig. 14). These Si atoms finally appear on the topmost surface layer, which is typically shown in graph (e) of 780°C in fig. 14.

5. Summary.

By using an analytical method for quantitative AES measurements, we determined the surface structures and their elemental compositions of a metal (Au, Cu or Pd) overlayer on a Si substrate at sequential heat-treatment steps. The main conclusions of this study can be summarized as follows:

(1) Au/Si system; At a heat-treatment temperature lower than the surface eutectic point (310°C), Si atoms which diffused from the substrate to the surface through the thick Au layer reacted with Au atoms to form the Au-silicide of a Au composition of 70 ∿ 85 at.% as the topmost layer. At a heat-treatment temperature higher than the surface eutectic point, the topmost Au layer of one to two monolayers was stably formed with a very abrupt interface on the Si substrate.

(2) Cu/Si system; At a heat-treatment temperature lower than 350 °C, Si atoms which diffused from the substrate to the surface through the deposited Cu layer formed the silicide Cu_3Si of the topmost layer, as was also the case with the Au/Si system at temperatures below the surface eutectic point. However, at a heat-treatment temperature higher than 350°C, we had different results from the Au/Si case. Instead of the sharp interface of Au/Si, we had the intermediate layer of Cu-Si alloy between the Cu surface layer and Si substrate, where the Cu composition gradually changed from 40 at.% to zero during heat-treatments.

(3) Pd/Si system; The interaction between the Pd film and the Si substrate took place even at 90°C, where Pd rich silicide was formed as Pd_2Si. At higher temperatures, the unit form of Pd_2Si diffused into Si or Si diffused among the Pd_2Si silicides. Finally, Si atoms segregated to the top surface of this silicide, due to the successive diffusion of Si from the Si substrate.

REFERENCES

[1] H. Tokutaka, K. Nishimori and K. Takashima, Surface Sci. 66 (1977) 659.

[2] H. Tokutaka, K. Nishimori and K. Takashima, Surface Sci. 86 (1979) 54.

[3] H. Tokutaka, K. Nishimori and K. Takashima, J. Appl. Phys. 50 (1979) 202.

[4] H. Tokutaka, K. Nishimori, K. Takashima, J. Le Hericy and J.P. Langeron J. Appl. Phys. 52 (1982) 6109.

[5] H. Tokutaka, K. Nishimori, S. Nomura, A. Tanaka and K. Takashima, Surface Sci. 115 (1982) 79.

[6] L. Braicovich, C.M. Garner, P.R. Skeath, C.Y. Su, P.W. Chye, I. Lindaw and W.E. Spicer, Phys. Rev. B20 (1979) 5131.

[7] I. Abbati and M. Ggrioni, J. Vac. Sci. Technol. 19 (1981) 631.

[8] N.W. Cheung, P.J. Grunthaner, F.J. Grunthaner, J.W. Mayer and B.M. Ullrich, J. Vac. Sci. Technol. 18 (1981) 917.

[9] P.S. Ho, P.E. Schmid and H. Foll, Phys. Rev. Letters 46 (1981) 782; and P.E. Schmid , P.S. Ho, H. Foll and G.W. Rubloff, J. Vac. Sci. Technol. 18 (1981) 937.

[10] J.A. Roth and C.R. Crowell, J. Vac. Sci. Technol. 15 (1978) 1317.

[11] J.T. Grant, T.W. Haas and J.E. Houston, J. Vac. Sci. Technol. 11 (1974) 227.

[12] K.L.I. Kobayashi, S. Sugaki, A. Ishizaka, Y. Shiraki, H. Daimon and Y. Murata, Phys. Rev. B25 (1982) 1377.

[13] K. Ishiguro and T. Homma, J. Jpn. Inst. Metals 45 (1981) 360 (in Japanese).

[14] H. Tokutaka, K. Nishimori, K. Takashima and T. Ichinokawa, Surface Sci. 133 (1983) 547.

[15] T. Narusawa, S. Komiya and A. Hiraki, Appl. Phys. Letters 22(1973) 389.

[16] A. Hiraki, M.A. Nicolet and J.W. Mayer, Appl. Phys. Letters 18 (1971) 178.

[17] A.K. Green and E. Bauer, J. Appl. Phys. 47 (1976) 1284.

[18] G. Lelay and J.P. Faurie, Surface Sci. 69 (1977) 295.

[19] F. Wehking, H. Beckermann and R. Niedermayer, Surface Sci. 71 (1978) 364.

[20] K. Oura and T. Hanawa, Surface Sci. 82 (1979) 202.

[21] T. Narusawa, K. Kinoshita and W.M. Gibson, J. Vac. Sci. Technol. 18 (1981) 872.

[22] C. Kittel, Introduction to Solid State Physics, 4th edition (John Wiley & Sons, New York, London, Sydney, Toronto, 1971), P 39.

[23] M. Hansen, in Constitution of Binary alloys (McGraw-Hill, New York, 1958), P. 629.

[24] G.Y. Robinson, Appl. Phys. Letters 25 (1974) 158.

[25] S. Okada, K. Oura, T. Hanawa and K. Satoh, Surface Sci. 97 (1980) 88.

[26] R.W. Bower, D. Sigurd and R.E. Scott, Solid State Electron. 16 (1973)1461.

[27] K.N. Tu, Appl. Phys. Letters 27 (1975) 221.

[28] J.L. Freeouf, G.W. Rubloff, P.S. Ho and T.S. Kuan, Phys. Rev. Letters 43 (1979) 1863.

[29] T.E. Gallon, J. phys. D5 (1972) 822.

[30] M. Gryzinski, Phys. Rev. A138 (1965) 336.